Heat Flow in the Central Gulf of California

LAWRENCE A. LAWVER[1]

Marine Physical Laboratory of the Scripps Institution of Oceanography, University of California, San Diego La Jolla, California 92093

DAVID L. WILLIAMS

U.S. Geological Survey, Denver, Colorado 80225

One hundred and five new heat flow measurements in the Gulf of California support the premise that conductive heat loss is not the only mode by which heat is lost from a sea floor spreading center, even in an area with thick sediment cover. Theoretical estimates suggest that the average heat flow in the Guaymas and Farallon basins should be at least 11 μcal/cm² s (HFU) (325 mW/m²). Outside a 30-km-wide zone centered on the central troughs, the heat flow values measured are reasonably uniform but average only 4.3 ± 0.2 HFU (180 ± 10 mW/m²). Although the high sedimentation rate may depress the measured heat flow, the effect probably does not exceed 15%. Some heat, particularly in the smaller basins, may be lost to the adjacent cooler continental blocks. The discrepancy between the measured and predicted heat losses, which is at least 30%, may be due to the discharge of thermal waters, through the thinner sediment cover in the central troughs or along active faults.

INTRODUCTION

Sea floor spreading is characterized by the intrusion of molten magma, which cools and contracts as it moves away from the spreading centers. High heat loss and elevated topography are predicted for the young crust near the axis of spreading, with both heat flow and elevation decreasing as the crust ages [*Sclater et al.*, 1971]. The East Pacific Rise at the mouth of the Gulf of California (Figure 1) is a typical spreading center, which shows a high heat loss, a decrease in elevation, and has easily correlatable magnetic anomalies [*R. L. Larson*, 1972]. To the south of the gulf the East Pacific Rise (EPR) is an extensional plate boundary, while to the north of the Gulf of California the right lateral strike slip motion along the prominent San Andreas transform fault system marks the plate boundary. A 300-km offset along the San Andreas [*Crowell*, 1973] can be documented. The trend of the gulf differs significantly from a small circle about the pole of rotation for the Pacific–North American plates, which is at 50.9°N, 66.3°W [*Minster et al.*, 1974]. The location of the pole requires an en echelon offset of the transform faults, and consequently, some form of crustal generation or sea floor spreading must be occurring in the gulf. The Gulf of California can be thought of as a transition zone between the normal sea floor spreading in the south and the predominantly transform faulting present in the north.

There is a lack of correlatable magnetic anomalies attributable to sea floor spreading in the Gulf of California. This is due in part to the thick sediment cover found in most of the basins [*R. L. Larson*, 1972]. Also, the seismic reflection results [*Moore*, 1973; *Bischoff and Henyey*, 1974; *Sharman*, 1976] are indicative of multiple sites of intrusion rather than a continuous nearly steady state type of intrusion. This would further tend to confuse any magnetic anomaly pattern; consequently, we must look to other direct evidence that supports active sea floor spreading. This paper concentrates on the central Gulf of California and examines what 146 measurements of conductive heat flow reveal about the development of the gulf.

[1] Now at U.S. Geological Survey, Menlo Park, California 94025.

Paper number 8B1126.

TECTONIC SETTING

The age and history of the gulf prior to the onset of transform faulting is not known definitively. *Ingle* [1973] found evidence for deepwater fauna in the northern gulf prior to 6 million years before present (m.y. B.P.). *Karig and Jensky* [1972] argued for a volcano-tectonic rift zone similar to the extensional zones behind many trench-arc systems along continental edges. *Atwater* [1970] showed that the last datable magnetic anomaly to the west of the Baja Peninsula is 11 m.y. B.P. (see Figure 1). If the gulf has been opening for only the last 4 m.y., then there must have been an interim period of 5–7 m.y. between cessation of spreading to the west and initiation of spreading in the gulf. During the interim period, shearing along the plate boundary may have accounted for the breakup of the continental borderland. Probably when that plate geometry became too difficult to sustain, the motion switched to the previously weakened Gulf of California. Because the trend of the protogulf [*P. A. Larson et al.*, 1972] did not conform to the direction of motion between the two major plates or because of a change in direction of motion, extensional rhomboid basins developed. *Shepard* [1950] and *Rusnak et al.* [1964] related the rhomboid shape of the basins to the strike slip motion of the faults. As the extensional region progresses further from a normal oceanic region and is offset by longer transform faults, the crust thickens [*Phillips*, 1964*a*], presumably influenced by the older and colder continental blocks.

MEASUREMENTS AND TECHNIQUES

One hundred and twenty-three heat flow measurements are reported in Tables 1-4. These values, plus 21 other published values not reported in the tables [*Lawver et al.*, 1973, 1975; *Von Herzen*, 1963], bring to 144 the number of published heat flow values in the central and southern Gulf of California. The values from the Guaymas, Carmen, and Farallon basins are plotted in Figures 2*a* and 2*b*. Two unpublished heat flow values (T. L. Henyey, personal communication, 1978) from the Guaymas basin outside the area of the figure are included in the comparison of heat flow with distance from the spreading center shown in Figure 3. Eighteen of the values in Table 1 are repeated from *Lawver et al.* [1973] because later measurements indicated that the values needed to be corrected for

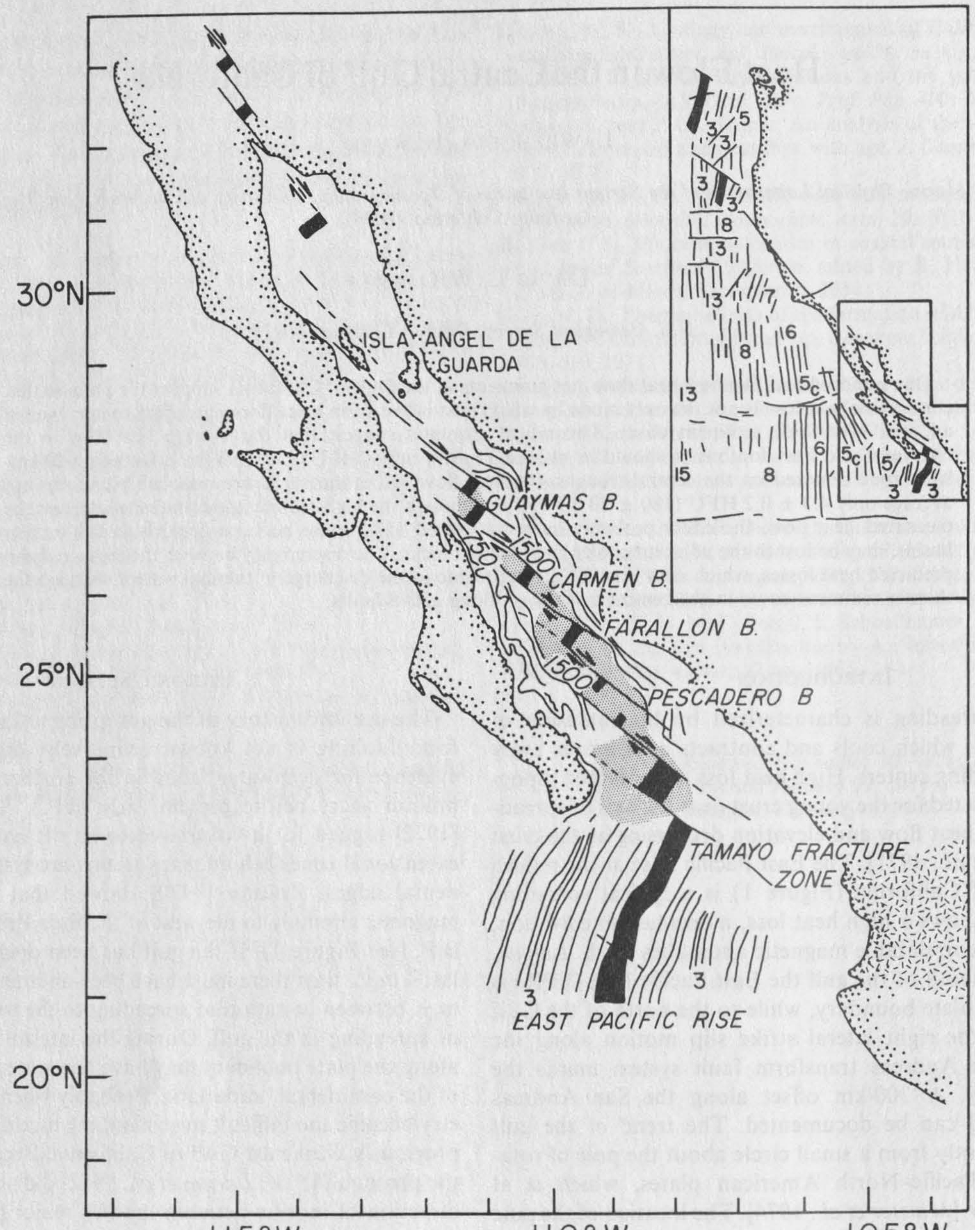

Fig. 1. Bathymetric contours and generalized tectonics of the Gulf of California. Contours are in uncorrected meters. The solid black areas represent possible spreading centers, the solid and dashed lines at right angles to these are fracture zones, and the light stippled areas are the enclosed basins [after *R. L. Larson,* 1972; *Lomintz et al.,* 1970, Figure 3]. The inset, which shows the distinctive magnetic lineations in the northwestern Pacific, has been taken from *Atwater* [1970]. The trans-Mexican volcanic zone is indicated by the andesitic intrusive pattern at 21°N, 103°W [after *Mooser,* 1972].

greater penetration than was originally assumed. Of the 144 thermal gradients, 52 were measured using the Woods Hole Oceanographic Institution's multipenetration heat flow probe [*Von Herzen and Anderson,* 1972], which consists of a 2.5-m probe with three outrigger thermistor probes at 1-m intervals. Acoustically telemetered data were recorded on a precision depth recorder. Seventy-nine of the thermal gradient measurements were taken using a 4.5-m-long Bullard-type probe [*Sclater et al.,* 1970]. Six 2-m Bullard-type probe measurements were taken, and seven measurements were made using outrigger thermistors attached to a 3-m gravity core barrel.

The Gulf of California has yet to be charted exactly because radar fixes give discrepancies of up to 5 km across the gulf. *Sharman* [1976] has revised bathymetric charts for parts of the Guaymas and Farallon basins, using satellite navigation data and radar ranges. His charts are the bases of Figures 4 and 5 and are supplemented with additional coverage using the older charts of *Rusnak et al.* [1964]. The depths found at each of the heat flow stations agree well with these hybrid charts. Some stations were located by using satellite navigation, but most were located by using radar fixes. Relative station location accuracy is probably better than 500 m. The detailed survey area A (Figure 2*b*) was navigated using a radar reflector whose position is shown as a cross on the top of the mound. Precisions of station locations for that survey are assumed to be 300 m or better.

Thermal conductivities of the gravity core and piston core samples reported by *Lawver et al.* [1973] were measured using the needle probe method of *Von Herzen and Maxwell* [1959]. Values ranged from 1.5×10^{-3} cal/°C cm s (0.63 W/mK) in

TABLE 1. Guaymas Basin Bullard Probe Heat Flow Measurements

	North Latitude	West Longitude	Depth, m	Bottom Temperature, °C	ΔT_1, °C	ΔT_2, °C	ΔT_3, °C	ΔT_4, °C	ΔT_{avg}	Penetration, cm	Q, μcal/cm^2 s (mW/m^2)	Tilt
HYPO-12	27°27.5′	111°22.7′	2038	2.889	OS	OS	OS	0.42	0.42	400	7.2(301)	V
HYPO-14	27°27.6′	111°23.5′	1886	2.885	0.45	0.33	0.35	0.35	0.35	430	6.0(252)	V
HYPO-15	27°31.2′	111°28.8′	1867	2.885	0.51	0.35	0.25	0.27	0.27	440	5.1(214)	V
HYPO-18	27°29.6′	111°26.7′	1871	2.883	0.28	0.18	0.18	0.17	0.18	455	3.1(130)	V
HYPO-61	27°28.3′	111°19.1′	1861	2.892	0.19	0.17	0.16	0.17	0.17	410	3.2(134)	15°–30°
HYPO-64	26°45.2′	110°49.7′	1662	2.859	0.25	0.24	0.24	0.24	0.24	400	4.1(170)	V
HYPO-65	26°44.4′	110°49.6′	1655	2.918	0.25	0.24	0.25	0.23	0.24	400	4.1(170)	V
VAL-1	27°28.5′	111°23.0′	2034	2.903	0.35	0.35	0.18	0.22	0.22	485	3.8(157)	15°–30°
VAL-2	27°15.0′	111°32.2′	2008	2.899	0.31	0.16	0.14	0.15	0.15	507	2.6(109)	V
VAL-3	27°19.2′	111°22.5′	1876	2.883	0.26	0.20	0.19	0.18	0.19	430	3.2(134)	V
VAL-4	27°22′	111°36.1′	1842	2.891	0.47	0.295	0.295	0.29	0.295	460	5.0(209)	V
VAL-5	27°25′	111°45′	1538	2.936	0.18	0.073	0.072	0.079	0.074	535	1.3(54)	V
VAL-7	26°56′	111°13.6′	1820	2.892	0.29	0.24	0.23	0.22	0.23	420	3.9(163)	V
VAL-8	27°03.3′	111°16.5′	1681	2.884	0.42	0.32	0.31	0.28	0.31	430	5.3(222)	V
EXT 1-1	27°25.4′	111°36.6′	1813	2.829	OS	OS	OS	0.40	0.40	>400	6.8(285)	V
EXT 1-2	27°21.8′	111°30.7′	1876	2.827	OS	OS	OS	0.39	0.39	>400	6.6(276)	V
EXT 1-3	27°18.7′	111°27.0′	1923	2.804	0.19	0.10	0.09	0.07	0.09	495	1.5(63)	V
EXT 1-5	27°37.0′	111°36.2′	1794	2.864	0.37	0.24	0.24	0.20	0.23	450	3.9(163)	V
EXT 1-6	27°24.6′	111°31.5′	1866	2.844	0.51	0.25	0.27	0.23	0.25	500	4.3(180)	V
EXT 1-7	27°26.3′	111°30.6′	1861	2.837	0.32	0.19	0.19	0.18	0.19	470	3.2(134)	V
EXT 1-8	27°31.5′	111°34.2′	1854	2.841	0.54	OS	0.35	0.30	0.32	470	5.5(230)	V
EXT 1-9	27°21.0′	111°22.4′	1846	2.806	0.51	OS	0.29	0.32	0.31	465	5.3(222)	V
EXT 1-10	27°22.8′	111°18.2′	1840	NT	NT	0.27	NT	NT	0.27	~460	4.6(193)	V
EXT 1-11	27°23.8′	111°13.7′	1831	2.836	0.41	0.30	0.30	0.26	0.30	435	5.1(214)	V
EXT 1-12	27°06.5′	111°27.7′	1907	2.822	0.12	0.23	0.22	0.19	0.22	350	4.1(170)	15°–30°
EXT 1-13	27°01.4′	111°32.9′	1815	2.851	0.21	0.20	0.19	0.17	0.19	405	~3.7(155)	>30°
EXT 1-14	27°02.1′	111°26.1′	2030	2.841	NP	NP	0.06	0.20	0.20	60?	~3.9(163)	>30°
EXT 1-15	27°08′	111°18′	1871	2.841	0.24	0.25	0.23	0.22	0.23	395	~4.5(188)	>30°
EXT 2-3	27°13.4′	111°15.2′	1865	2.844	0.28	0.21	0.21	0.18	0.21	435	3.6(151)	V
EXT 2-4	27°02.8′	111°25.0′	2026	2.878	OS	OS	OS	OS	>0.7	>400	>14.0(586)	V
EXT 2-5	27°03.9′	111°06.6′	1764	2.846	0.29	0.23	0.23	0.22	0.23	425	3.9(163)	V
EXT 2-6	27°13.7′	110°55.5′	1548	2.861	0.02	0.22	0.17	0.17	0.17	310	~3.3(138)	>30°
EXT 2-7	27°05.0′	110°52.0′	1584	2.88	0.05	0.25	0.21	0.22	0.22	320	~4.3(180)	>30°
EXT 2-8	26°57.8′	110°59.3′	1689	2.880	0.31	0.29	0.29	0.28	0.29	405	5.0(209)	V
EXT 2-9	26°55.0′	110°46.5′	1574	1.886	0.33	0.25	0.23	0.22	0.23	435	3.9(163)	V
EXT 2-10	26°49.2′	110°54.2′	1717	2.847	0.29	0.27	0.26	0.25	0.26	405	4.5(188)	V
EXT 2-37	26°40.8′	110°54.5′	1692	2.846	0.18	0.43	OS	0.45	0.45	345	~8.8(368)	>30°
EXT 2-38	26°51.3′	111°03.7′	1784	2.847	0.37	0.32	OS	0.32	0.32	415	~6.3(264)	>30°
EXT 2-39	26°57.5′	111°25.5′	2040	2.863	0.23	0.15	0.16	0.14	0.15	450	~2.9(121)	>30°
EXT 2-42	27°21.1′	111°29.7′	2010	2.857	OS	OS	OS	0.31	0.31	>400	5.8(243)	15°–30°
EXT 2-43	27°31.1′	111°22.4′	2045	2.851	0.41	0.20	0.20	0.17	0.20	510	3.8(159)	15°–30°
EXT 2-44	27°18.0′	111°05.0′	1707	2.834	0.28	0.24	0.22	0.21	0.22	420	~4.3(180)	>30°
7404-1	28°28.7′	111°22.6′	2051	2.935	0.26	0.11	0.11	0.11	0.11	530	1.8(75)	V
7404-2	27°27.4′	111°22.8′	2048	2.910	0.24	0.11	0.11	0.09	0.11	520	1.8(75)	V
7404-3	27°27.9′	111°22.7′	2053	2.903	OS	OS	0.36	0.36	0.36	>400	7.1(279)	15°–30°
7404-4	27°03.1′	111°25.4′	1970	2.906	NP	0.07	0.13	0.11	0.12	255	2.4(100)	15°–30°
7404-5	27°03.1′	111°25.4′	1970	2.901	NP	0.04	0.08	0.10	0.10	240	2.0(84)	15°–30°
7404-6	27°31.0′	111°21.6′	2052	2.911	0.55	0.20	0.21	0.9	0.20	570	3.4(142)	V
7404-7	27°32.6′	111°23.0′	2020	2.884	0.42	0.20	0.21	0.17	0.20	505	8.9(163)	15°–30°

OS means off scale (data segments were off scale, indicating a thermal gradient larger than we could measure). V means vertical, i.e., <15° tilt. NT means that no trace for that data segment appeared on the record. NP means no penetration. A value of ~3.7 indicates that the probe penetrated at an angle of >30°, the measured value was corrected by +15%.

the top layer of most of the cores to 2.21 × 10^{-3} cal/°C cm s (0.93 W/mK) in a dense sandy layer in a core taken at the mouth of the gulf near the East Pacific Rise. All of the conductivities in the central gulf below the top 50 cm were between 1.62 and 1.75 × 10^{-3}cal/°C cm s (0.68–0.73 W/mK). At each Bullard probe station a 10-cm core was taken, which showed that the surface sediments in the gulf are reasonably uniform and consist almost exclusively of a foram rich, green hemipelagic mud.

The heat flow values listed in Tables 1-4 are the product of the measured thermal gradients and thermal conductivities from nearby cores. For Tables 1 and 2 an assumed thermal conductivity of 1.71 × 10^{-3}cal/°C cm s (0.71 W/mK) was used, except for stations HYPO-64 and HYPO-65, where a normal oceanic thermal conductivity of 2.0 × 10^{-3}cal/°C cm s (0.84 W/mK) was assumed because of the more compact nature of the sediments in the core taken nearby. For the stations in the Farallon basin (Table 3) a thermal conductivity of 1.75 × 10^{-3}cal/°C cm s (0.73 W/mK) was assumed. The miscellaneous stations in Table 4 have the conductivities listed. The heat flow instruments have two tilt indicators. One indicates >30° tilt, and the other indicates between 15° and 30° tilt. In the case of the instrument being tilted less than 15°, it is listed in the tables as having been vertical. If the instrument tilted between 15° and 30°, then a 10% correction was added to the measured heat flow value; a 15% correction was applied when tilts exceeded 30°. Obviously, the thermal gradients might actually be much higher than calculated values if the

TABLE 2. *Agassiz* 7410 Heat Flow Measurements From a Detailed Survey in Northeast Guaymas Depression

Station	Depth, m	Bottom Temperature, °C	ΔT_1, °C/m	ΔT_2, °C/m	ΔT_{avg}, °C/m	Q, μcal/cm² s (mW/m²)	Tilt
Detailed Survey in Northern Guaymas Trough							
7410-1	2041	2.848	0.12	0.13	0.13	2.1(88)	V
7410-2	2041	2.839	0.12	0.13	0.13	2.1(88)	V
7410-3	2048	2.853	0.13	0.12	0.13	2.1(88)	V
7410-4	2003	2.846	0.16	0.16	0.16	2.8(117)	V
7410-5	1964	NWT	0.18	0.18	0.18	3.3(138)	15°–30°
7410-6	2018	NWT	NA	0.36	0.36	5.9(247)	V
7410-7	1976	2.837	0.19	0.20	0.20	3.4(142)	V
7410-8	1980	2.803	0.13	0.15	0.14	2.6(109)	15°–30°
7410-9	2026	2.839	0.19	0.25	0.25	4.3(180)	V
7410-10	1996	2.977	OS	0.41	0.41	7.0(293)	V
7410-11	1967	2.839	OS	0.38	0.38	≥7.7(322)	>30°
7410-12	1937	2.839	0.21	0.25	0.25	≥5.0(209)	>30°
7410-13	1923	2.832	0.18	0.22	0.22	≥4.3(180)	>30°
7410-14	2015	2.832	0.24	0.24	0.24	4.1(172)	V
7410-15	2019	2.841	0.22	0.24	0.23	4.4(184)	15°–30°
7410-16	2034	2.846	0.21	0.24	0.22	4.2(176)	15°–30°
7410-17	2039	2.844	0.21	0.21	0.21	3.6(151)	V
7410-18	2039	2.844	0.18	0.21	0.20	3.3(138)	V
7410-19	2028	2.844	0.17	0.20	0.19	≥3.7(155)	>30°
7410-20	2017	NWT	0.23	0.21	0.22	≥4.3(180)	>30°
7410-21	1985	2.830	0.18	0.18	0.18	≥3.5(147)	>30°
7410-22	1978	2.841	0.21	0.24	0.22	4.2(174)	15°–30°
7410-23	1967	2.841	0.31	0.31	0.31	≥6.0(252)	>30°
7410-24	2041	2.846	0.12	0.10	0.11	1.8(75)	V
7410-25	2041	2.846	0.16	0.12	0.14	2.7(114)	15°–30°
7410-26	2036	2.851	0.12	0.13	0.13	≥2.5(109)	>30°
7410-27	2015	2.849	0.21	0.18	0.19	≥3.5(147)	>30°
7410-28	1992	2.841	0.22	0.21	0.22	≥4.2(174)	>30°
7410-29	2030	2.849	0.10	0.13	0.13	2.2(92)	V
7410-30	1908	2.845	0.11	0.11	0.11	≥2.1(88)	>30°
7410-31	1894	2.849	0.23	0.23	0.23	4.4(185)	15°–30°
7410-32	1894	2.834	NP	0.15	0.15	≥2.9(121)	>30°
7410-33	1893	2.827	0.38	0.38	0.38	≥7.5(313)	>30°
Profile Across Probable Fracture Zone at 111°30′W, 27°10′N							
7410-34	1958	2.856	0.52	0.52	0.52	8.8(369)	V
7410-35	1957	2.859	0.41	0.35	0.38	6.4(268)	V
7410-36	1959	2.830	0.35	0.30	0.32	5.8(243)	V
7410-37	1957	2.851	0.38	0.39	0.38	5.7(238)	V
7410-38	1946	2.851	0.35	0.57	0.46	7.4(309)	15°–30°
7410-39	1967	2.857	0.42	0.42	0.42	7.1(297)	15°–30°
7410-40	1969	2.853	0.59	0.59	0.59	10.0(419)	V
7410-41	1973	2.860	0.46	0.46	0.46	7.9(331)	V
7410-42	1961	NWT	0.53	0.53	0.53	9.1(381)	V

Data are Woods Hole Oceanographic Institution multipenetration heat flow measurements in the Guaymas basin. Stations 7410-1–7410-33 are from a detailed survey in the northern Guaymas trough (see Figure 2*b* for locations). Stations 7410-34–7410-42 are a profile of heat flow values taken across a probable transform fault at 111°30′W, 27°10′N (see Figure 4 for locations). V means verticle, i.e., <15° tilt; NWT means no water temperature recorded; NA means not available; OS means off scale; NP means no penetration; and ≥7.7 indicates that the probe penetrated at a >30° angle, the measured value corrected by +15%.

probe penetrated at a >45° angle from vertical, but it is assumed, given the characteristics of the unconsolidated sediments and the dynamics of a probe being lowered, that the instrument would have fallen over and no usable value would have been observed. This occurred only once.

In addition to heat flow measurements, bottom water thermal gradients were measured at selected localities in the gulf using two different devices towed near the sea floor. The first device consisted of two separate heat flow packages (without probes) bolted together such that the two water temperature thermistors were 2 m apart. The package was towed as close to the bottom as was practical, using a Benthos pinger for navigation. No temperature anomaly was observed. The second temperature-monitoring device was a modified AMF temperature telemetering pinger with three thermistors at the ends of 1-, 5-, and 10-m cables. Again the instrument was towed at speeds of approximately 1–2 kn (2–3.5 km/h), and no temperature anomalies were detected.

HEAT FLOW IN THE GUAYMAS AND FARALLON BASINS

The heat flow measurements in the Guaymas and Farallon basins were all taken in at least 1500 m of water (Figure 2*a*) and on sediments overlying what is assumed to be young oceanic crust (Figure 2*a*). Within each of the two basins is a central trough perpendicular to active transform faults. If the central trough is the site of the most recent spreading, then we might expect the highest conductive heat flow to be found there if the thick sediment cover is acting as an impermeable

TABLE 3. Farallon Basin Bullard Probe Heat Flow Measurements

	North Latitude	West Longitude	Depth, m	Bottom Temperature, °C	ΔT_1, °C	ΔT_2, °C	ΔT_3, °C	ΔT_4, °C	ΔT_{avg}, °C	Penetration, cm	Q, μcal/cm² s (mW/m²)	Tilt
HYPO-2	25°11.1′	109°27.5′	2024	NT	0.24	0.20	NA	NA	0.20	220	3.5(147)	V
HYPO-5	25°23.5′	109°54.6′	3204	NT	0.19	0.16	NA	NA	0.16	220	2.8(117)	V
HYPO-6	25°26.2′	109°44.8′	2230	NT	0.35	0.21	0.24	0.24	0.24	445	4.2(176)	V
HYPO-9	25°32.8′	109°47.3′	3182	NT	0.21	0.17	0.18	0.17	0.17	420	3.1(130)	V
HYPO-55	25°21.4′	109°42.0′	2193	NT	0.64	OS	OS	0.42	0.42	450	7.1(297)	V
HYPO-66	25°19.3′	109°48.5′	2335	2.262	0.20	0.44	OS	0.43	0.44	345	~8.9(373)	>30°
EXT 2-14	25°40.8′	110°06.2′	2242	NT	0.37	0.27	0.26	0.24	0.26	435	4.6(193)	V
EXT 2-15	25°29.3′	109°57.0′	2022	2.281	0.38	0.29	0.29	0.26	0.29	430	5.1(214)	V
EXT 2-16	25°30.4′	109°59.0′	1987	2.238	0.36	OS	OS	0.49	0.49	375	~9.9(415)	>30°
EXT 2-17	25°35.4′	109°50.5′	2178	2.234	NP	PP	OS	0.30	0.30	>200	~6.1(255)	>30°
EXT 2-18	25°29.7′	109°45.0′	2438	2.267	0.48	OS	OS	0.35	0.35	435	~7.0(293)	>30°
EXT 2-20	25°15.0′	109°39.0′	2236	2.233	0.13	0.25	0.24	0.25	0.25	350	~5.0(209)	>30°
EXT 2-22	25°12.6′	109°38.2′	2248	NT	0.07	0.21	0.20	0.18	0.20	330	3.8(159)	15°–30°
EXT 2-23	25°15.5′	109°45.2′	2310	2.208	0.06	0.35	OS	0.48	0.48	275	~9.7(406)	>30°
EXT 2-24	25°21.0′	109°40.0′	2205	NT	0.08	0.33	OS	0.34	0.34	325	~6.8(285)	>30°
EXT 2-25	25°23′	109°36′	2068	2.234	0.22	0.20	0.20	0.18	0.20	410	~4.0(167)	>30°
EXT 2-26	25°25.5′	109°38.2′	2105	NT	0.20	0.21	0.21	0.22	0.21	395	~4.2(176)	>30°
EXT 2-27	25°21.6′	109°49.0′	2365	NT	NOS	0.25	NOS	NOS	0.25	~400	~4.4(184)	?
EXT 2-28	25°24.6′	109°56.8′	3202	NT	0.35	0.26	0.29	0.26	0.26	435	~5.2(218)	>30°
EXT 2-32	25°36.7′	110°02.2′	2330	NT	0.22	0.17	0.16	0.13	0.16	425	3.1(130)	15°–30°
EXT 2-33	25°33.3′	110°16.3′	2070	NT	0.27	0.20	0.19	0.17	0.19	435	3.3(138)	V
7404-8	25°20.3′	109°41.4′	2240	2.257	OS	OS	OS	OS	OS	>400	>16. (670)	15°–30°

V means vertical, i.e., <15° tilt; NT means that no trace for that data segment appeared on the record; OS means off scale; and ~8.9 indicates that the probe was at a >30° angle (the measured value was corrected by + 15%).

layer. Assuming no other heat loss mechanism and regardless of the nature of spreading, if all the crustal extension has taken place within the basin boundaries and in a reasonably continuous manner, then the average heat flow for each basin should be in the range predicted by theoretical cooling models [e.g., *Sclater and Francheteau,* 1970; *Parker and Oldenburg,* 1974; *Parsons and Sclater,* 1977]. The conductive heat flow that we observed, shown in Figures 4 and 5, is not in this range. Figure 6 shows the expected theoretical heat flow values for a uniform basin 4 m.y. old and assumes no heat loss to the cold continental blocks.

Some of the most pertinent observations are as follows:

1. The average conductive heat flow for the two basins is similar. For all the measurements, including minimum values, the means and standard errors for the Guaymas basin and Farallon basin are 5.3 ± 0.4 HFU and 5.8 ± 0.7 HFU, respectively. If we exclude all maximum and minimum values because they might be simply reflecting very local thermal anomalies, the averages are still similar: 4.3 ± 0.2 HFU for the Guaymas basin and 4.6 ± 0.3 HFU for the Farallon basin.

2. The conductive heat flow distributions in the two basins are different (Figures 3 and 7). In the Guaymas basin the highest heat flow values are found in the central trough, whereas in the Farallon basin they are found 15–20 km from either side of the axis of the central trough.

3. The averages of the heat flow profiles in Figures 3 and 7 indicate that the conducted heat flow is less than two thirds of the heat flow predicted by the sea floor spreading model of *Sclater and Francheteau* [1970]. If we use $q = 11.3/t^{1/2}$, where t is in millions of years [*Parsons and Sclater,* 1977], and integrate it to find the amount of heat lost between 0 and 4 m.y., we get $\int_0^4 q\,dt = 22.6t^{1/2}|_0^4 = 45.2\,\mu$cal/cm², or an average heat flow of 11.3 HFU. If we exclude the very young crust between 0 and 0.5 m.y. in order to give our theoretical average a conservative bias, the result is 8.2 HFU. For very young crust an average of over 30 HFU would be expected, and while values this high have been found, an average of all our values on very young crust would not be anywhere near this value.

TABLE 4. Other Bullard Probe Heat Flow Measurements

	North Latitude	West Longitude	Depth, m	Bottom Temperature, °C	ΔT_1, °C	ΔT_2, °C	ΔT_3, °C	ΔT_4, °C	ΔT_{avg}, °C	Penetration, cm	K, cal/°C cm s (W/m °K)	Q, μcal/cm² s (mW/m²)	Tilt
HYPO-22	28°42.3′	113°03.6′	1572	11.34	−0.08	OS	0.13	0.13	0.13	350	1.65(0.69)	2.3(96)	15°–30°
HYPO-26	28°46.5′	113°05.3′	1370	11.34	−0.06	OS	−0.04	−0.02	−0.04	450	1.67(0.69)	−0.6(−25)	V
HYPO-40	26°23.3′	110°44.9′	2785	NT	0.32	0.16	0.16	0.15	0.16	490	1.68(0.70)	2.7(113)	V
EXT 2-11	26°20.6′	110°45.2′	2804	2.549	0.11	−0.01	−0.01	−0.01	−0.01	>400	1.68(0.70)	−0.2(−8)	V
EXT 2-12	26°13.3′	110°40.7′	2456	2.513	NP	0.14	0.21	0.19	0.20	265	1.68(0.70)	~3.9(173)	>30°
EXT 2-34	25°54.3′	110°13.8′	2032	2.519	PP	PP	PP	0.12	0.12	57	2.0(0.84)	2.7(113)	V
EXT 2-35	26°07′	110°29′	2333	2.492	0.04	0.12	0.12	0.12	0.12	330	1.68(0.70)	2.4(100)	V
EXT 2-36	26°21.9′	110°46.0′	2758	2.540	0.43	0.26	0.28	0.25	0.26	470	1.68(0.70)	4.4(184)	V
HYPO-68	23°27.7′	108°20.7′	2651	1.810	OS	OS	OS	0.35	0.35	>400	2.0(0.84)	7.0(293)	V
HYPO-69	23°02.1′	107°59.6′	2584	1.799	0.14	0.12	0.10	0.11	0.11	430	2.0(0.84)	2.2(92)	V

Data are Bullard probe heat flow measurements from other basins and the East Pacific Rise. V means vertical, i.e., <15°. NP means no penetration; NT means no trace; OS means off scale; and ~3.9 indicates that the probe penetrated at a >30° angle (the measured value was corrected by +15%). PP means partial penetration.

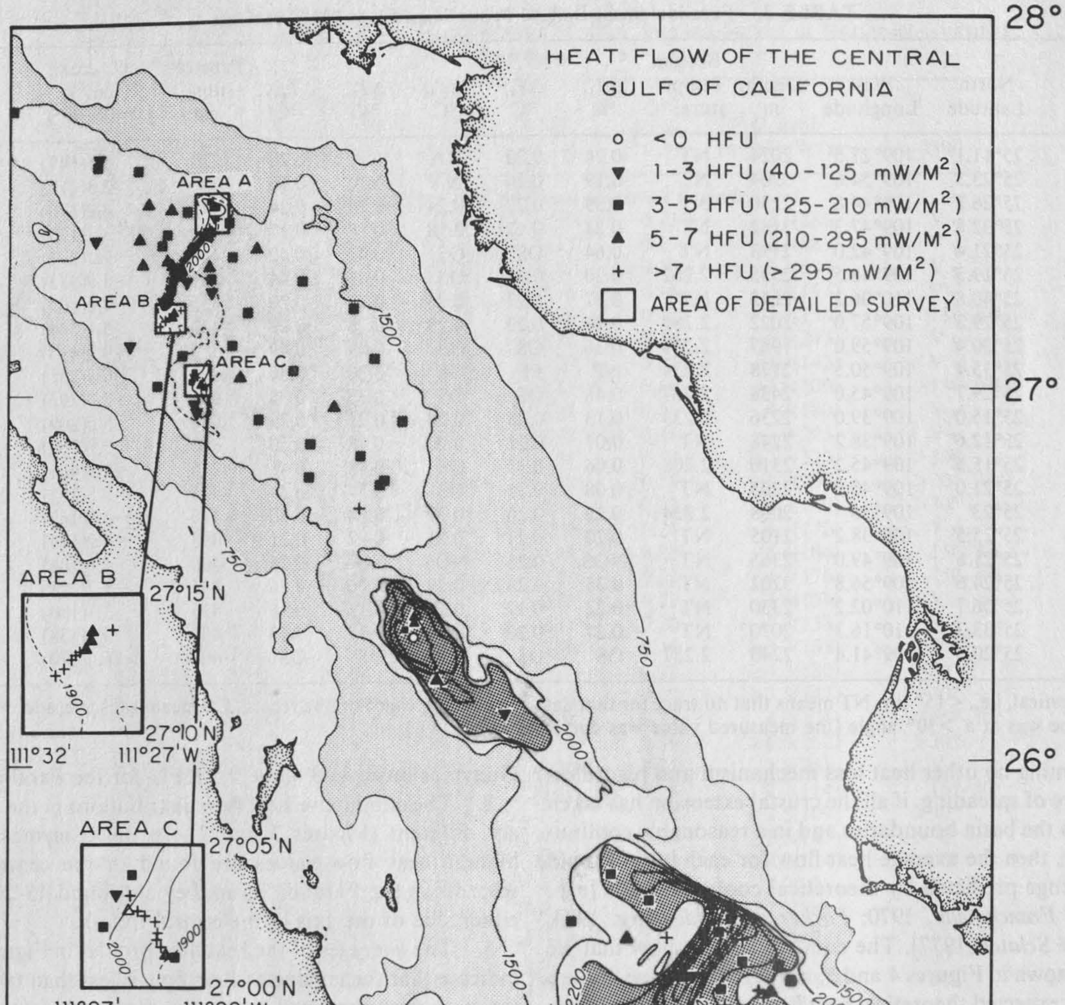

Fig. 2a. Chart of heat flow measurements from the Farallon, Carmen, and Guaymas basins. Contours are in uncorrected meters [from *Sharman,* 1976; *Rusnak et al.,* 1964].

Because there are no correlated magnetic anomalies, the distribution of very young crust is uncertain near the present spreading centers.

4. There is a large scatter in measured heat flow values in both basins (Figure 8). It is not uncommon to find values differing by a factor of 2 or 3 within a few hundred meters of each other, particularly in the central trough in the Guaymas basins (Figure 3) and 20 km south of the central trough in the Farallon basin (Figure 7).

5. Both basins are generally covered by several hundred meters of sediment; however, there are exceptions. Areas that have thin sediments and basement outcrops are found along the transform faults bounding the basins, as well as along the north wall of the central trough in the Farallon basin and around a few isolated basement highs throughout the central gulf.

THERMAL EFFECTS OF SEDIMENTATION

The discharges of the rivers to the east of the gulf, together with productivity of the Gulf of California, cause the central basins to have high sedimentation rates. *Calvert* [1966] inferred four sedimentation rates for the Guaymas basin from radiocarbon dating of core sections and found rates of 0.23 and 2.76 m/1000 years in the southern parts of the basin and 4.71 and 4.98 m/1000 years in the extreme northern part. He also measured a rate of 1 m/1000 years in the Farallon basin. Using a ^{210}Pb method, *Bruland* [1974] studied the sedimentation rate in the northern Guaymas basin and reported a rate of 1.5 m/1000 years; a rate of 1.6 m/1000 years was found by counting varves in the same box core. These high sedimentation rates appear to be inconsistent with the age and observed total sediment thickness of the gulf. Seismic reflection profiles [*Phillips,* 1964*b*, Figure 4; *Moore,* 1973] suggest a maximum sediment thickness of only about 1 km. A sedimentation rate of 0.4 m/1000 years with a 30% compaction estimate would produce 1 km of sediment in 4 m.y. This is much less than the high rates measured in either the Guaymas or the Farallon basin. We do not know how to account for this discrepancy. A more reasonable sedimentation history might be 1.5 m/1000 years for the last 100,000 years, and perhaps a fluctuating rate

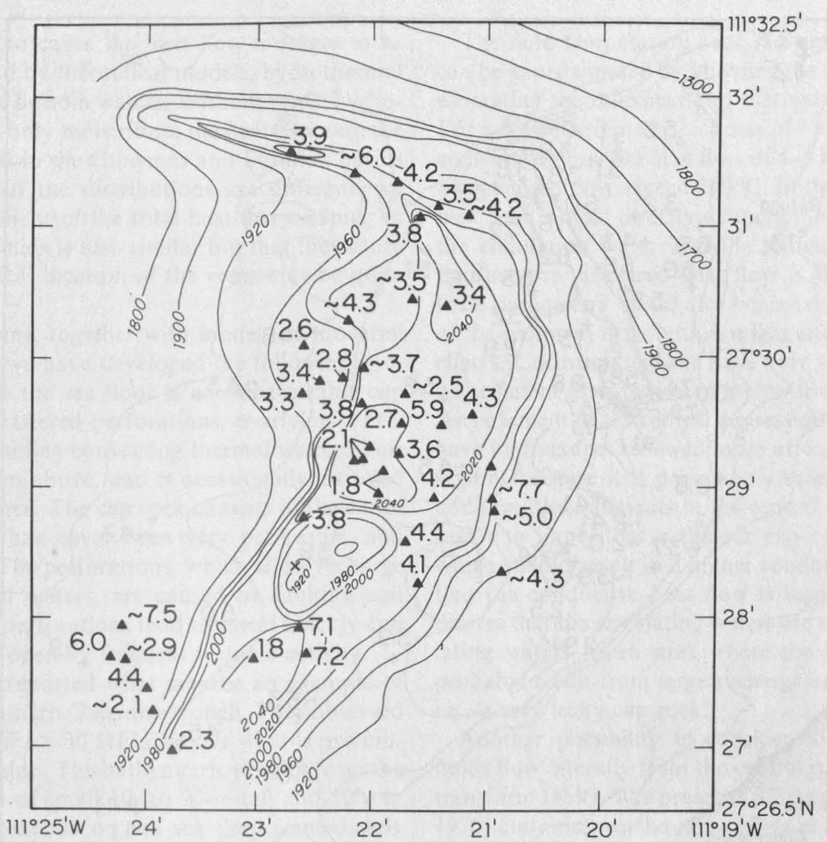

Fig. 2*b*. Detailed survey area A of the northeast Guaymas depression showing a centrally located mound rising 100 m from the floor of the depression. Heat flow values are in μcal/cm² (1 μcal/cm² s = 41.78 mW/m²). Contours are in uncorrected meters.

prior to that, to give a total of approximately 1 km of consolidated sediment in 4 m.y., or an average rate of 0.5 m/1000 years.

High sedimentation rates have a pronounced effect on the observed thermal gradient because of the absorption of heat by the rapidly accumulating sediments. Temperatures in the crust must also adjust to the changing location of the sediment-water interface. The result is time dependent and can produce a substantial reduction in near-surface thermal gradients. The more rapid the sedimentation, and the longer the sedimentation history, the more the thermal gradient is depressed. Where heat transfer is only by conduction, reliable estimates of this effect can be made [*Von Herzen and Uyeda,* 1963]. If the high rates discussed above (4.71 and 4.98 m/1000 years) had persisted for 100,000 years, they would have reduced the measured gradient to approximately 30% of the equilibrium values. However, if we take an average rate of only 0.5 m/1000 years or the higher rate of 1.5 m/1000 years for a short recent period, the observed thermal gradient is reduced to approximately 90% of equilibrium.

One more possibility should be mentioned. If what was interpreted as basement in the seismic reflection surveys is, in fact, not basement but metamorphosed sedimentary rocks, the actual sediment thickness and sedimentation rates could be much larger than we assumed, and their effect on the thermal gradient could be much larger. Preliminary results from a multichannel seismic reflection survey of the gulf indicate that the assumed sediment thickness estimates are correct.

Finally, if convection is the dominant mode of heat transfer, the high sedimentation rates in the gulf would still tend to reduce the observed heat flow. Simple analytical estimates of the effect are not possible, but as with conduction, the new sediments must be heated, and crustal temperature must adjust to the new location of the sediment-water interface. Convection, being a more efficient form of heat transfer, should allow the adjustment to be accomplished more rapidly.

It is clear from this discussion that the correction to measured thermal gradients required to account for sedimentation

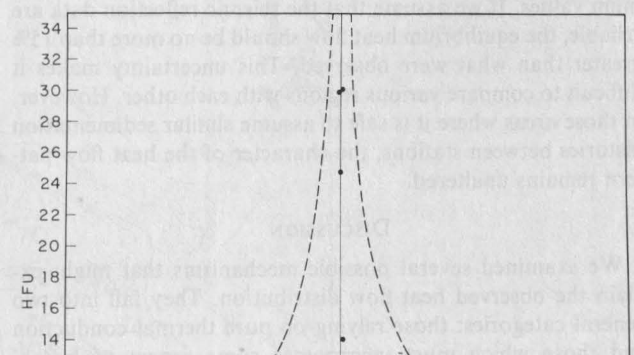

Fig. 3. Plots of Guaymas basin heat flow values versus distance from the central depression.

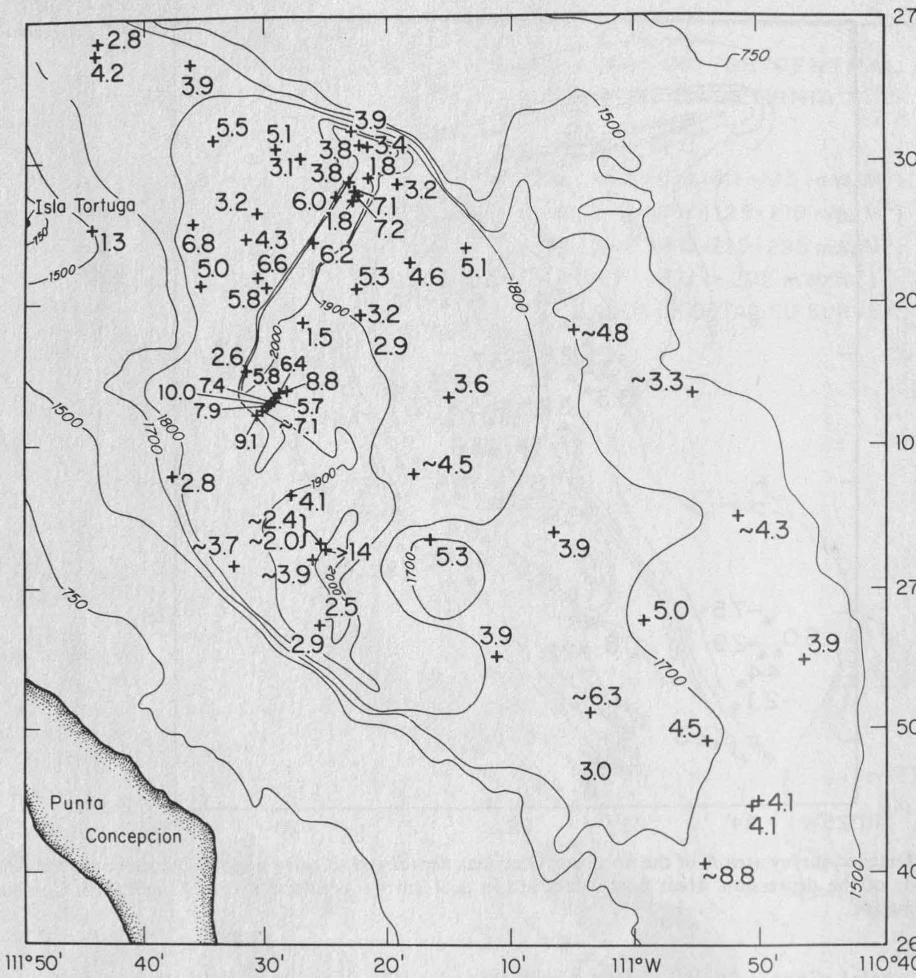

Fig. 4. Guaymas basin heat flow values omitting the Woods Hole Oceanographic Institution's multipenetration probe values shown in Figure 2*b* of this paper and in Figure 2 of *Lawver et al.* [1975]. Contours are in meters and are from *Sharman* [1976] and *Rusnak et al.* [1964]. Heat flow values are in $\mu cal/cm^2$ s.

could be substantial, but because of the large uncertainties involved we cannot make this correction with confidence. No corrections have been attempted, and the measured heat flows in the Guaymas and Farallon basins must be considered minimum values. If we assume that the seismic reflection data are reliable, the equilibrium heat flow should be no more than 15% greater than what were observed. This uncertainty makes it difficult to compare various regions with each other. However, in those areas where it is safe to assume similar sedimentation histories between stations, the character of the heat flow pattern remains unaltered.

DISCUSSION

We examined several possible mechanisms that might explain the observed heat flow distribution. They fall into two general categories: those relying on pure thermal conduction and those which must incorporate some aspect of hydrothermal circulation. In the first category are the following mechanisms:

1. Thermal refraction. This may cause variations of up to 50% in some extreme localities [*Sclater et al.*, 1970] but is small for most of our stations in comparison with the observed variations in heat flow.

2. Bottom water temperature variations. These can cause large disturbances in the near-surface thermal gradients [e.g., *Williams et al.*, 1977]; however, we find no evidence of anomalous bottom water conditions.

3. Turbidity currents or slumping of sediments. The bathymetry [*Sharman*, 1976] leads us to the conclusion that this is not an important process outside of the central troughs. The Farallon central trough may have severely reduced surface heat flux due to slumping.

4. Heat source variability. This effect can cause a scatter in data, but the total amount of heat released via thermal conduction would remain unchanged, so it cannot explain the discrepancy between predicted and observed heat flows.

5. High sedimentation rates. As was discussed earlier, rapidly accumulating sediments can suppress the heat flow. However, because the greatest discrepancies between measured and predicted heat flows occur near the presumed centers of spreading (i.e., the central troughs) where the sediments are thinnest and, consequently, the sedimentation effect the least [*Von Herzen and Uyeda*, 1963], it seems unlikely that the sedimentation can account for more than a small part of the discrepancy between measured and predicted fluxes.

6. A final possibility is that the age of the Gulf of California is twice that which is assumed (i.e., 8 m.y. old instead of 4 m.y.). This seems difficult to accept because the magnetic anomalies at the mouth of the gulf effectively span the width of the gulf and are dated as 0–4 m.y.

Because none of these effects can adequately explain our observations, the answer must apparently be found in the second category, that is, a heat transfer mechanism which incorporates some form of hydrothermal circulation. For hydrothermal circulation to cause the heat flow averages to be less than those predicted by theoretical models, hydrothermal fluids must vent into the bottom waters. Without vents, hydrothermal circulation can only redistribute the heat. Because the average heat flow values in the Guaymas and Farallon basins are nearly the same but the distributions are different, we assume that the component of the total heat flux escaping in venting hydrothermal fluids is also similar but that the nature of the systems and typical location of the vents may be quite different.

Using our observations, together with models of subaerial hydrothermal systems, we have developed the following conceptual model: Beneath the sea floor is an impermeable cap rock that has widely scattered perforations, overlying a permeable formation containing convecting thermal waters. This permeable formation lies above, and is occasionally intruded by, an igneous heat source. The cap rock consists of the entire sediment layer, which has never been very permeable, and some basement rocks. The perforations, which allow recharge and venting of thermal waters, are caused by faulting and igneous activity. These perforations tend to reseal quickly and therefore must be kept open by frequent tectonic activity.

Lawver et al. [1975] reported what may be an example of such a system in the southern Guaymas trough. They observed extremely high heat flow (> 30 HFU) above what is presumably a very recent intrusion. The bathymetric profiles from the region reveal a number of small 10- to 20-m-tall and 100- to 200-m-wide sediment mounds on the sea floor immediately above the intrusion. These may be analogous to the hydrothermal mounds found near the Galapagos spreading center by *Klitgord and Mudie* [1974] and *Williams et al.* [1974].

The fluid temperature near the top of the convecting layer can be approximated by knowing the conductive heat flow and estimating the thickness and thermal conductivity of the cap. For a typical sediment thickness of 1 km in the central gulf and an average observed heat flow of 4–5 HFU, fluid temperatures would commonly exceed 200°C. In this model, the conductive heat flow is most directly a function of the depth to the top of the circulating water and the temperature of those waters. Because the measured heat flow is variable, one or both of these parameters would also be variable. Adequate knowledge of the sediment distribution might enable us to separate these effects. Unfortunately, we have only very general information on sediment distribution in the central gulf. We would expect the basement of the central depression of the Farallon basin to have its fractures renewed more often than the more outlying regions because it is presumably more tectonically active. In addition, the sediments in the central region are thinner. This seems to imply that a thinner cap rock would be expected, which should result in a higher conductive heat flow. The fact that the conductive heat flow is lower instead of higher indicates that the circulating waters are much cooler. Cool circulating waters in an area where the total heat flow is high probably result from large recharge and discharge flow rates, i.e., a very leaky cap rock.

Another possibility to consider is that the hydrothermal fluids flow laterally from the central parts of the basins to the transform faults. The presence of impressive scarps [*Sharman*, 1976] and microearthquakes [*Reid et al.*, 1973] indicates that these faults are active. Other investigators [*Sclater et al.*, 1974; *Lister*, 1976] have suggested large lateral flows from beneath sediment areas to basement outcrops. *Lister* [1976] describes a

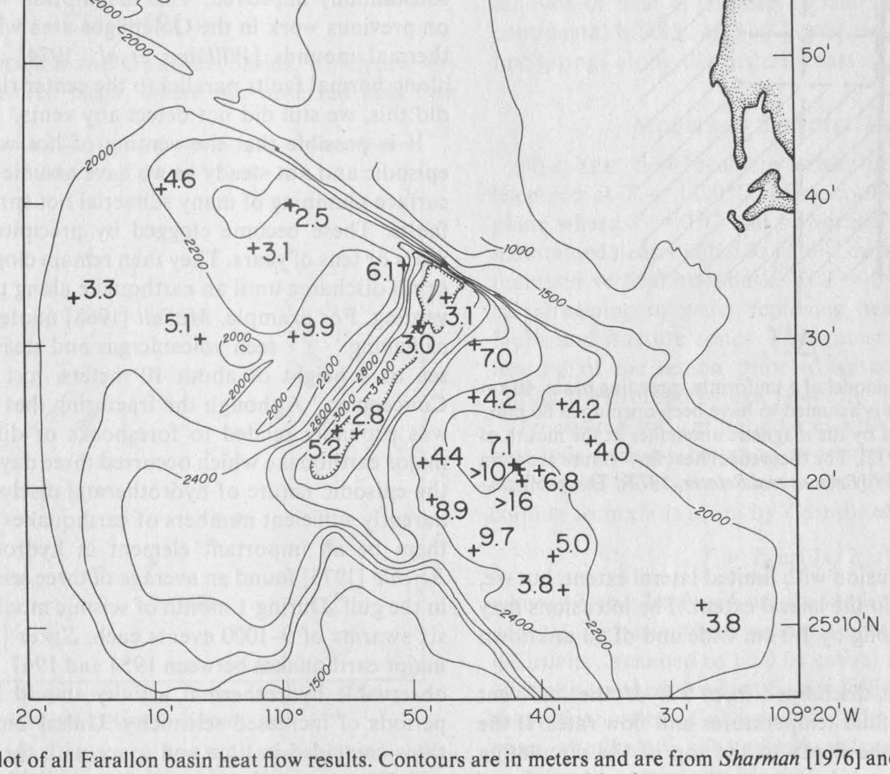

Fig. 5. Plot of all Farallon basin heat flow results. Contours are in meters and are from *Sharman* [1976] and *Rusnak et al.* [1964]. Heat flow values are in $\mu cal/cm^2$ s.

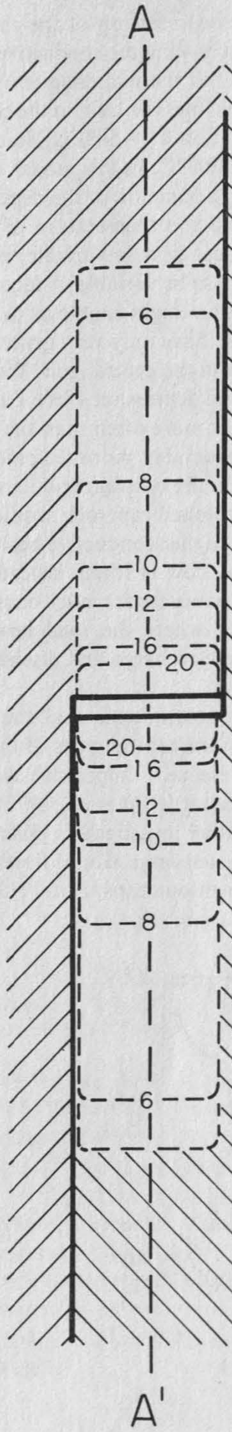

Fig. 6*a*. A simplified model of a uniformly spreading basin, 40 km wide and 240 km long. It is assumed to have been opening at 60 mm/yr for 4 m.y. as suggested by the magnetic anomalies at the mouth of the gulf [*R. L. Larson*, 1972]. The theoretical heat flow values are from the equation $Q = 11.3/t^{1/2}$ [*Parsons and Sclater*, 1977]. The profile A-A′ is shown in Figure 6*b*.

three-dimensional intrusion with limited lateral extent, but we, in fact, are interested in the lateral extent. The intrusions may be as much as 20 km long by 1.0 km wide and of an unknown thickness.

The amount of heat discharged from a hydrothermal vent depends primarily on fluid temperatures and flow rates. If the total flux is 8 HFU, the depth to the top of the circulating water system is 1 km, and the average thermal conductivity of this cap is 2×10^{-3} cal/cm s °C, then the escaping hydrothermal fluids may be responsible for removing approximately 4 HFU. If one spring occurred every 1 km², it would discharge at a rate of about 0.2 l/s at a temperature somewhat below 200°C. For one spring every 10 km² or 100 km² the flow rates would increase to 2 and 20 l/s, respectively. These are modest flow rates relative to subaerial hot springs. Water from such vents should be buoyant and rise, rapidly mixing with the bottom waters. The resulting bottom water thermal anomaly should attenuate to less than 0.01°C within a few tens of meters of the vent.

To search for vents, we towed bottom water temperature sensors for about 50 km in and near the central trough of the northeastern Guaymas basin. If we assume that one, and only one, vent occurs somewhere in each 1 km² and that its detection radius is 20 m, then on an average we would have to tow for 25 km to locate the vent. If the detection radius is some factor more or less than 20 m, then the distance is changed by the reciprocal of that factor. The reverse is true if we change the size of the unit area, as is seen in this simplified equation:

$$D r_d N / A = P$$

where

- D distance traveled;
- r_d detection radius;
- N number of springs per unit area;
- A unit area;
- P probability of detection.

Thus by towing 50 km, our chance of success was good only if there are many springs, e.g., one per square kilometer, each with a detection radius of greater than 10 m.

We felt that the springs were probably not as randomly scattered as the above calculations assume. If vents tend to occur near faults, and we biased our experiment toward probable faults, then our chances of success should have been substantially improved. This assumption was partially based on previous work in the Galapagos area where known hydrothermal mounds [*Williams et al.*, 1974] are found lineated along normal faults parallel to the center rift. Even though we did this, we still did not detect any vents.

It is possible that the venting of hot water is variable or episodic and not steady as we have assumed above. The near-surface plumbing of many subaerial hot springs is provided by faults. These become clogged by precipitates in a very few years or tens of years. They then remain clogged and have little or no discharge until an earthquake along the fault renews the venting. For example, *McFall* [1968] quotes his field assistant as having '· · · seen volcanic gas and steam rising out of the sea to a height of about 10 meters, just offshore of Bahia Concepcion.' Although the fracturing that vented these fluids was probably related to foreshocks or dilation prior to the major earthquake which occurred three days later, it illustrates the episodic nature of hydrothermal discharge. There are apparently sufficient numbers of earthquakes in the gulf to have them be an important element in hydrothermal discharge. *Reichle* [1975] found an average of three seismic events per day in the gulf. During 1 month of seismic monitoring he observed six swarms of 9–1000 events each. *Sykes* [1968] reported five major earthquakes between 1954 and 1967. It seems likely that observable hydrothermal activity should be associated with periods of increased seismicity. Unless our thermal observations coincided in time and space with the vent locations and with the associated seismicity, it is probable that we would not

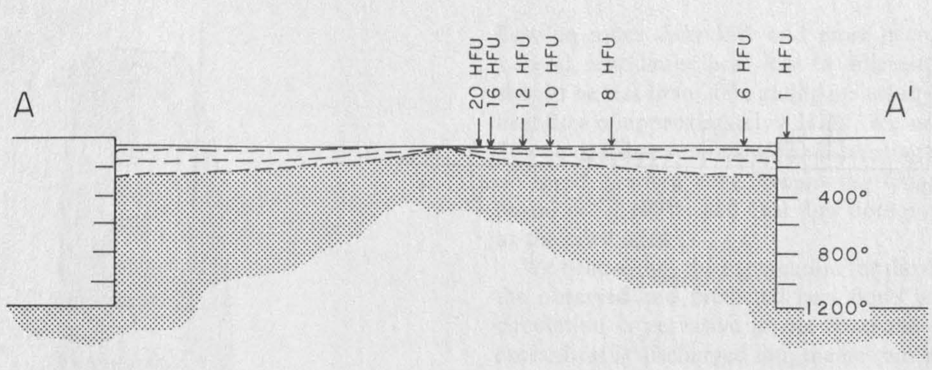

Fig. 6*b*. A profile perpendicular to the assumed spreading center between points A and A' shown in Figure 6*a*. The model assumes steady state constant spreading, although the Guaymas basin really shows evidence of jumped centers of spreading. The stippled region represents presumed mantle material at 1200°C.

see them. As was found on the Galapagos rift zone, the vents appear episodic even in an active normal oceanic rift [*Crane and Ballard*, 1979]. In the Guaymas basin the whole circulating system is complicated by the thick sediment cover.

Recently, Lonsdale and Lawver dove on four sites in the central troughs of the Guaymas basin in the U.S. Navy submersible *Seacliffe* (the work will be reported by P. F. Lonsdale et al. (unpublished data, 1979)). They report that the floors of the troughs are generally covered with soft fine sediment. On 3.5-kHz records the regions of the troughs that are covered with fine sediment show one or more acoustically transparent layers, 5–10 m thick. Two dives were made in the one central trough region that did not show the transparent layers. The bottom was very rough, and an apparently inactive but recent probable hydrothermal vent was found on one of the dives. These findings tend to substantiate the idea that hydrothermal vents are episodic and are not as numerous as those found in other areas such as the Galapagos spreading center. It is still probable that most of the hydrothermal heat loss may occur along faults and would not be detected as mounds or show up as possible sites on 3.5-kHz records.

CARMEN BASIN

Between the Farallon and Guaymas basins, which are very similar, is the Carmen basin, where our observed heat flow values are low and scattered. The six values measured in the basin (Table 4) give a median heat flow of 2.7 HFU and include a negative heat flow value of −0.2 HFU shown as an open circle on Figure 2*a*. The negative value is most likely an indication of a recent slump or a recent bottom water temperature increase. A very low heat flow value may result from hydrothermal circulation, but not a negative value. The Carmen basin, in contrast to the Farallon and Guaymas basins, is less than 20 km wide between transform faults. The length of the basin is 90 km compared to the 240 km of the Farallon and Guaymas basins, so it cannot have had the same spreading history as the other two basins. *Crowell* [1975] postulated formation of long narrow basins caused by bends in transform faults. A bend in the transform fault between the Guaymas and Farallon basins might be responsible for the development of the Carmen basin. *Sharman* [1976] proposed a model in which the initiation of the Carmen basin was at about 0.7 m.y. B.P. but with an episodic history that included at least three distinct spreading episodes.

Because the Carmen basin is much narrower than either the Guaymas or the Farallon basin, it is possible that a significant amount of heat is transferred laterally to heat the adjacent continental blocks. *McFall* [1968] reported a number of very hot springs along the eastern coast of Baja California.

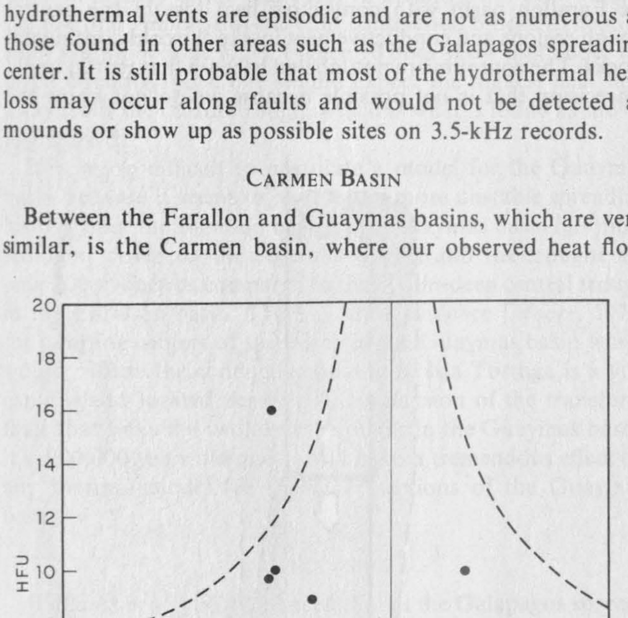

Fig. 7. Plot of Farallon basin heat flow values versus distance from the central depression.

MODELS OF EXPECTED HEAT FLOW

This heat flow problem might be modeled as a parallelepiped at $T = 1200°C$, being cooled both by a horizontal plane where $T = 0°C$ and by vertical boundaries where T is maintained nearly equal to zero [*Lawver*, 1976, pp. 67–71]. To maintain vertical boundaries at $T = 0°C$, there must be vertical streaming of water removing heat along the transform faults and fracture zones. There must also have been no preheating of the region prior to initiation of spreading, i.e., during the protogulf stage 11–4 m.y. B.P.

To assume vertical boundaries with $T = 0°C$ is unrealistic, and it is perhaps better to show the possible effect of cold continental blocks by a simple approximation. The half-space cooling formula is given by *Carslaw and Jaeger* [1959, p. 59]:

$$T = T_0 \operatorname{erf} [x/2(\kappa t)^{1/2}]$$

where x is the distance from the vertical boundary forming the edge of the basin which acts as a heat sink, t is time, and κ is diffusivity, assumed to be 0.01 cm²/s. For t = 1 m.y. and x = 10 km the conductive heat flow would be reduced to 79% of its theoretical value. Consequently, almost the entire Carmen basin would show substantially reduced heat flow due to loss to the cold continental blocks.

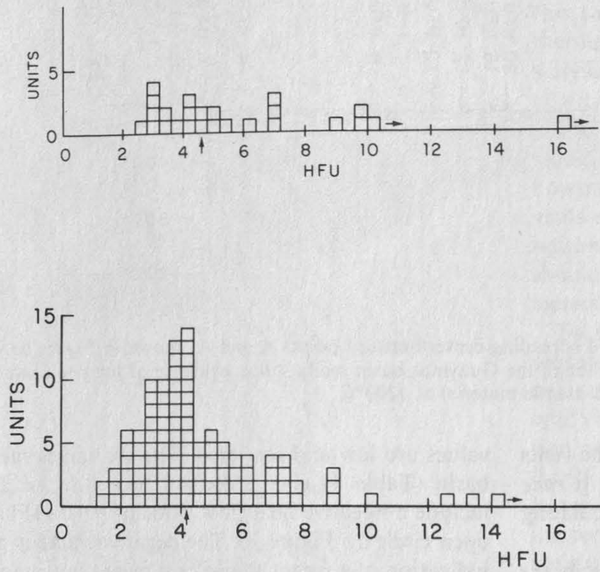

Fig. 8. Histograms of the Farallon and Guaymas basins heat flow values in μcal/cm² s. The upper histogram shows 25 values from the Farallon basin, of which one value is >10 HFU and another >16 HFU. The median value for the Farallon basin appears to be 4.5 HFU. The lower histogram shows 110 values from the Guaymas basin, of which one value was off scale but >14 HFU. The median value for the Guaymas basin appears to be 4.1 HFU.

The larger Guaymas and Farallon basins should show a heat loss to the cold continental blocks only around the edges during the first 1 m.y. The larger basins would have to be cooled laterally for 3 m.y. before the same percentage of cooling would be seen as is seen at 1 m.y. in the Carmen basin and similar smaller basins. If the Carmen basin is very young and the area around it was not preheated by protogulf activity, then the percentage of heat loss to the cold continental blocks should be substantially more than the percentage lost by the larger Guaymas and Farallon basins. Lateral conductive heat loss should be less than 20% of the total heat released as a result of the sea floor spreading process, bringing the theoretical heat flow average to ~8 HFU after the warming of the sediment is considered.

Figure 6 shows the expected theoretical heat flow based on the *Parsons and Sclater* [1977] model but does not allow for the warming of cold continental blocks. If we assume that the horizontal heating effect will be felt at a distance approximated by $l = (4\kappa t)^{1/2}$ with t being time and κ diffusivity, then the horizontal heating from the new oceanic crust will be 11.2 km for a time of 1 m.y. Figure 9 shows qualitatively the expected heating of the continental blocks for a basin 40 km wide and having spread for 4 m.y. at 30 mm/yr. The primary heating effect is caused by the ridge having been in contact with the continental crust. The secondary heating is due to the warm oceanic lithosphere being in contact with the cold continental lithosphere. As can be seen in Figure 9, the primary heating effect is greatest at the ends of the basin where the oceanic and continental crusts have been in stable contact since the basin first opened. The primary heating effect decreases along the inactive fracture zones as one nears the spreading center. Along the active transform fault the continental crust has never been primarily heated by the spreading ridge. The extent of the heating effect and the time of heating decrease away from the spreading center until the far north and south corners of the basin are in contact with cold unheated continental crust. All along the stable fracture zones the continental blocks have been either primarily or secondarily heated for the whole age of the basin.

If, as is suspected, the Farallon basin loses a lot of heat convectively along the steep walls of the central trough, then Figure 9 should be modified to show low heat flow in the central trough due not only to the convective loss but also to the suppressed heat flow because of high sedimentation from turbidity currents and slumping. Figure 10 shows a model of the Farallon basin with convective heat loss in the central trough regions and conductive heat loss to the cold continental blocks. The contours are not labeled because that would imply a precision that is not possible because we do not know the

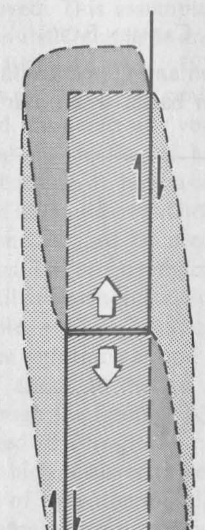

Fig. 9. Heating of cold continental blocks. The hatched area represents new oceanic crust. The dark stippled region represents primarily heated continental crust, while the light stippled area represents secondarily heated continental regions. The single solid lines represent active transform faults, while the double solid line represents an active spreading center.

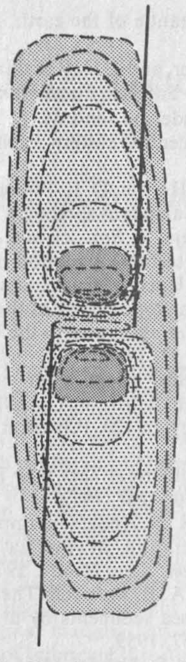

Fig. 10. Model for the Farallon basin. The dark stippled areas represent regions of highest conductive heat flow. The light stippled areas represent regions of moderate conductive heat flow, and the medium stippled areas represent regions of lower conductive heat flow. The central trough between the two solid lines representing active transform faults would have low conductive heat flow because of convective heat loss through the unsedimented north wall of the trough and because of slumping of sediments into the deep central trough. The dashed lines are generalized contour lines of heat flow.

thermal history of the gulf prior to opening; nor do we know the thermal response of the cold continental blocks to heating from young oceanic crust. Figure 10 does show that under the given circumstances, one should expect the highest heat flow away from the central trough, which is what is found as shown in Figure 5.

It is more difficult to postulate a model for the Guaymas basin because it seems to have had a more unstable spreading history than the Farallon basin. The Guaymas basin has more sediment cover on the central troughs, and the troughs are only 200 m deep as compared to the 800-m-deep central trough in the Farallon basin. There is some evidence [*Moore,* 1973] for jumping centers of spreading in the Guaymas basin which would diffuse the conductive heat loss. Isla Tortuga is a volcanic island located nearly on an extension of the transform fault that links the two central troughs in the Guaymas basin; it is 900,000 years old and would have a tremendous effect on any thermal model for the older sections of the Guaymas basin.

CONCLUSION

Williams et al. [1974] deduced that at the Galapagos spreading center, 50 m or more of sediment effectively sealed the upper boundary of the hydrothermal circulation system and stopped the convective loss of heat. In these more heavily sedimented areas they measured heat flow that approximated the predicted heat flow of *Sclater and Francheteau* [1970]. Because of its thick sedimentary cover we expected a similar situation in the Gulf of California. The basins of the central Gulf of California, greater than 1000 m deep, appear to be less than 4 m.y. old. Therefore we expected these basins to have an average heat flow of greater than 11 HFU. The high sedimentation rate in the gulf probably suppresses the observed heat flow no more than 15% and more probably closer to 10%. Lateral conductive heat loss to adjacent continental blocks should be less than 20%, giving an adjusted predicted average heat flow of approximately 8 HFU. We would also expect heat flow to decrease smoothly with increasing age of the crust. The observed average heat flow in the Guaymas and Farallon basins is 5.7 HFU, and heat flow does not smoothly decrease as the crust ages.

We believe that the explanation for the discrepancy between the observed and predicted heat flows is that hydrothermal circulation is pervasive in the basement rocks and that the excess heat is discharged into the bottom water through warm springs. Most of the discharge presumably takes place near the central troughs, since the discrepancy between observed and predicted heat flows is much less on crust older than 500,000 years.

Acknowledgments. The measurements listed in the tables were collected with the help of many people, including C. Down, J. Rogers, J. Hunt, K. Green, and R. Zuck. M. Reichle and G. Sharman helped organize the Exito cruises and participated in them. R. P. Von Herzen lent us the WHOI heat flow equipment. R. Schwartzlose provided us with ship time on the R/V *Agassiz.* V. Vacquier, J. Sclater, and R. P. Von Herzen have all commented on the manuscript. The Mexican government kindly extended us permission to work in their waters. This study was supported primarily by grants from the U.S. National Science Foundation, NSF GA-38072 and GA-31704. Contribution of the Scripps Institution of Oceanography, new series.

REFERENCES

Atwater, T., Implications of plate tectonics for the Cenozoic tectonic evolution of western North America, *Geol. Soc. Amer. Bull., 81,* 3513, 1970.

Bischoff, J. L., and T. L. Henyey, Tectonic elements of the central part of the Gulf of California, *Geol. Soc. Amer. Bull., 85,* 1893, 1974.

Bruland, K., Pb-210 geochronology in the coastal marine environment, Ph.D. thesis, 68 pp., Univ. of Calif., San Diego, 1974.

Calvert, S. E., Accumulation of diatomaceous silica in the sediments of the Gulf of California, *Geol. Soc. Amer. Bull., 77,* 569, 1966.

Carslaw, H. S., and J. C. Jaeger, *Conduction of Heat in Solids,* 510 pp., Oxford University Press, New York, 1959.

Crane, K., and R. D. Ballard, Galapagos rift at 86°W, 4, Structure and morphology of hydrothermal fields and their relationships to the volcanics and tectonic processes of the rift valley, submitted to *J. Geophys. Res.,* 1979.

Crowell, J. C., Problems concerning the San Andreas fault system in southern California, in *Proceedings of the Conference on Tectonic Problems of the San Andreas Fault System, Publ. Geol. Sci. XIII,* p. 125, Stanford University, Stanford, Calif., 1973.

Crowell, J. C., Sedimentation along the San Andreas fault, California, *Soc. Econ. Paleontol. Mineral. Spec. Publ., 19,* 292, 1975.

Ingle, J. C., Jr., Neogene marine history of the Gulf of California: Foraminiferal evidence, *Geol. Soc. Amer. Abstr. Programs, 5,* 62, 1973.

Karig, D., and W. Jensky, The proto-gulf of California, *Earth Planet. Sci. Lett., 17,* 169, 1972.

Klitgord, K. D., and J. D. Mudie, The Galapagos spreading centre: A near-bottom geophysical survey, *Geophys. J. Roy. Astron. Soc., 38,* 563, 1974.

Larson, P. A., J. D. Mudie, and R. L. Larson, Magnetic anomalies and fracture zone trends in the Gulf of California, *Geol. Soc. Amer. Bull., 83,* 3361, 1972.

Larson, R. L., Bathymetry, magnetic anomalies, and plate tectonic history of the Gulf of California, *Geol. Soc. Amer. Bull., 83,* 3345, 1972.

Lawver, L. A., Heat flow in the Gulf of California, Ph.D. thesis, 76 pp., Univ. of Calif., San Diego, 1976.

Lawver, L. A., J. G. Sclater, T. L. Henyey, and J. Rogers, Heat flow measurements in the southern portion of the Gulf of California, *Earth Planet. Sci. Lett., 19,* 198, 1973.

Lawver, L. A., D. L. Williams, and R. P. Von Herzen, A major geothermal anomaly in the Gulf of California, *Nature, 257,* 23, 1975.

Lister, C. R. B., Qualitative theory on the deep end of geothermal systems, in *Second U. N. Symposium on the Development and Use of Geothermal Resources*, p. 459, U.S. Government Printing Office, Washington, D. C., 1976.

Lomnitz, C., F. Mooser, C. R. Allen, J. N. Brune, and W. Thatcher, Seismicity and tectonics of the northern Gulf of California region, Mexico: Preliminary results, *Geofis. Int., 10*(2), 37, 1970.

McFall, C. C., Reconnaissance geology of the Concepcion Bay area, Baja, California, Mexico, *Stanford Univ. Publ. Geol. Sci., X*(5), 25 pp., 1968.

Minster, J. B., T. H. Jordan, P. Molnar, and E. Hains, Numerical modelling of instantaneous plate tectonics, *Geophys. J. Roy. Astron. Soc., 36,* 25, 1974.

Moore, D. G., Plate-edge deformation and crustal growth, Gulf of California structural province, *Geol. Soc. Amer. Bull., 84,* 1883, 1973.

Mooser, F., The Mexican volcanic belt: Structure and tectonics, *Geofis. Int., 12*(2), 55, 1972.

Parker, R. L., and D. W. Oldenburg, Thermal model of ocean ridges, *Nature Phys. Sci., 242,* 137, 1973.

Parsons, B., and J. G. Sclater, An analysis of the variation of ocean floor bathymetry and heat flow with age, *J. Geophys. Res., 82,* 803–827, 1977.

Phillips, R. P., Seismic refraction studies in the Gulf of California, in *Marine Geology of the Gulf of California, Mem. 3,* p. 90, American Association of Petroleum Geologists, Tulsa, Okla., 1964*a*.

Phillips, R. P., Gepohysical investigations in the Gulf of California, Ph.D. thesis, 250 pp., Univ. of Calif., San Diego, 1964*b*.

Reichle, M. S., A seismological study of the Gulf of California: Sonobuoy and teleseismic observations, and tectonic implications, Ph.D. thesis, 249 pp., Univ. of Calif., San Diego, 1975.

Reid, I., M. Reichle, J. Brune, and H. Bradner, Microearthquake studies using sonobuoys: Preliminary results from the Gulf of California, *Geophys. J. Roy. Astron. Soc., 34,* 365, 1973.

Rusnak, G. A., R. L. Fisher, and F. P. Shepard, Bathymetry and faults of the Gulf of California, in *Marine Geology of the Gulf of California, Mem. 3,* p. 59, American Association of Petroleum Geologists, Tulsa, Okla., 1964.

Sclater, J. G., and J. Francheteau, The implications of terrestrial heat-flow observations on current tectonic and geochemical models of the crust and upper mantle of the earth, *Geophys. J. Roy. Astron. Soc., 20,* 509, 1970.

Sclater, J. G., V. Vacquier, and J. H. Rohrhirsch, Terrestrial heat-flow measurements of Lake Titicaca, *Earth Planet. Sci. Lett., 8,* 45, 1970.

Sclater, J. G., R. N. Anderson, and M. L. Bell, Elevation of ridges and evolution of the central eastern Pacific, *J. Geophys. Res., 76,* 7888, 1971.

Sclater, J. G., R. P. Von Herzen, D. L. Williams, R. N. Anderson, and K. D. Klitgord, The Galapagos spreading centre: Heat-flow low on the north flank, *Geophys. J. Roy. Astron. Soc., 38,* 609, 1974.

Sharman, G., The plate tectonic evolution of the Gulf of California, Ph.D. thesis, 100 pp., Univ. of Calif., San Diego, 1976.

Shepard, F. P., Submarine topography of the Gulf of California, Part 3 of the 1940 *E. W. Scripps* cruise to the Gulf of California, *Geol. Soc. Amer. Mem., 43,* 32, 1950.

Sykes, L. R., Seismological evidence for transform faults, sea-floor spreading, and continental drift, in *The History of the Earth's Crust,* edited by R. A. Phinney, p. 120, Princeton University Press, Princeton, N. J., 1968.

Von Herzen, R. P., Geothermal heat flow in the gulfs of California and Aden, *Science, 140,* 1207, 1963.

Von Herzen, R. P., and R. N. Anderson, Implications of heat flow and bottom water temperature in the eastern equatorial Pacific, *Geophys. J. Roy. Astron. Soc., 26* 427, 1972.

Von Herzen, R. P., and A. E. Maxwell, The measurement of thermal conductivity of deep-sea sediments by a needle probe method, *J. Geophys. Res., 64,* 1557, 1959.

Von Herzen, R. P., and S. Uyeda, Heat flow through the eastern Pacific Ocean floor, *J. Geophys. Res., 68,* 4219, 1963.

Williams, D. L., R. P. Von Herzen, J. G. Sclater, and R. N. Anderson, The Galapagos spreading centre: Lithospheric cooling and hydrothermal circulation, *Geophys. J. Roy. Astron. Soc., 38,* 587, 1974.

Willams, D. L., T. C. Lee, R. P. von Herzen, K. E. Green, and M. A Hobart, A geothermal study of the Mid-Atlantic Ridge near 37°N, *Geol. Soc. Amer. Bull., 88,* 531, 1977.

(Received August 15, 1978;
revised September 11, 1978;
accepted October 20, 1978.)